

Reduction of Target Gene Expression by a Modified U1 snRNA

S. A. BECKLEY,¹ P. LIU,¹ M. L. STOVER,¹ S. I. GUNDERSON,² A. C. LICHTLER,¹ AND D. W. ROWE^{1*}

Department of Genetics and Developmental Biology, University of Connecticut Health Center, Farmington, Connecticut 06030,¹ and Department of Molecular Biology and Biochemistry, Rutgers University, Piscataway, New Jersey 08854²

Received 3 August 2000/Returned for modification 28 September 2000/Accepted 17 January 2000

Although the primary function of U1 snRNA is to define the 5' donor site of an intron, it can also block the accumulation of a specific RNA transcript when it binds to a donor sequence within its terminal exon. This work was initiated to investigate if this property of U1 snRNA could be exploited as an effective method for inactivating any target gene. The initial 10-bp segment of U1 snRNA, which is complementary to the 5' donor sequence, was modified to recognize various target mRNAs (chloramphenicol acetyltransferase [CAT], β -galactosidase, or green fluorescent protein [GFP]). Transient cotransfection of reporter genes and appropriate U1 antitarget vectors resulted in >90% reduction of transgene expression. Numerous sites within the CAT transcript were suitable for targeting. The inhibitory effect of the U1 antitarget vector is directly related to the hybrid formed between the U1 vector and target transcripts and is dependent on an intact 70,000-molecular-weight binding domain within the U1 gene. The effect is long lasting when the target (CAT or GFP) and U1 antitarget construct are inserted into fibroblasts by stable transfection. Clonal cell lines derived from stable transfection with a pOB4GFP target construct and subsequently stably transfected with the U1 anti-GFP construct were selected. The degree to which GFP fluorescence was inhibited by U1 anti-GFP in the various clonal cell lines was assessed by fluorescence-activated cell sorter analysis. RNA analysis demonstrated reduction of the GFP mRNA in the nuclear and cytoplasmic compartment and proper 3' cleavage of the GFP residual transcript. An RNase protection strategy demonstrated that the transfected U1 antitarget RNA level varied between 1 to 8% of the endogenous U1 snRNA level. U1 antitarget vectors were demonstrated to have potential as effective inhibitors of gene expression in intact cells.

Reducing the output of a target gene has a prominent role in therapeutic strategies for heritable diseases resulting from a dominant negative mutation and in assessing gene function during development. While inactivation at the level of the gene is most definitive, current approaches are time-consuming (22, 62) or are still in early stages of development (19, 43). Targeting the mRNA transcripts of a specific gene with antisense oligonucleotides (77) or genes that express an antisense RNA (67) or a ribozyme (39) has shown variable success. Since no clear effector design has proven to be superior, new strategies are continually being introduced. In particular, imbedding the antisense or ribozyme effector within expression loci of snRNA or tRNA genes is proving to have a distinct advantage of high expression and nuclear localization (8). For example, an anti-HIV ribozyme imbedded within a U1 snRNA-derived vector reduced the expression of HIV RNA transcripts by 60% within *Xenopus laevis* oocytes (59). Subsequently, stable transfection of the same effector into Jurkat cells dramatically reduced intracellular HIV transcript levels (58). Ribozymes incorporated into the U1 snRNA gene reduced fibrillin 1 gene expression in cell culture (60). Antisense delivered within the U7 snRNA gene inhibited the expression of aberrantly spliced β -globin mRNA by 60% in a β -thalassemia cell line (79). Neuregulin-1 was significantly reduced in developing chick embryos by expression of multiple ribozymes imbedded in a tRNA

gene and delivered to the chick in the context of a replication competent retrovector (85). Further improvements in the design of the chimeric tRNA-ribozyme construct have increased catalytic activity (46, 57).

Here, we report an alternative approach for reducing the mRNA output of a target gene using a modified U1 snRNA transcript as the effector. The first 10-nt of the human U1 snRNA gene, which normally binds to 5'ss (CAGIGTAAGTA [vertical bar shows splice site]) in pre-mRNA (6, 34, 48, 61), were replaced by a sequence complementary to a 10-nt segment in the terminal exon of the target mRNA. While this U1 targeting strategy, like ribozyme and antisense methods, depends on the formation of an RNA-RNA hybrid, a mechanism different from antisense mediated RNase H destruction (26), antisense mediated inosine substitutions (44), or ribozyme cleavage (51, 80) is utilized. Rather, binding of the U1 snRNA effector to a terminal exon appears to interfere with posttranscriptional processing of that transcript, resulting in reduced accumulation of that mRNA (23, 37). U1 snRNA is a component of the U1 snRNP complex, which also contains seven common snRNP proteins and three specific U1 snRNP proteins (73, 74, 83). It initiates spliceosome association with pre-mRNA by defining the 3' boundary of exons (71). As the splicing reaction proceeds, U1 snRNP and the other spliceosome components are sequentially released from the transcript (41).

Factors that affect the dissociation of U1 snRNP from a transcript have been found to control mRNA expression in several natural and engineered situations. Persistent binding of U1 snRNA to a β -globin transcript containing a mutant splice donor site is postulated to account for low β -globin accumu-

* Corresponding author. Mailing address: Department of Genetics and Developmental Biology, Mail Code 1231, University of Connecticut Health Center, 263 Farmington Ave., Farmington, CT 06030. Phone: (860) 679-2324. Fax: (860) 679-8345. E-mail: drowe@nso1.uhc.edu.

lation in certain forms of β -thalassemia (10). Failure of the splicing reaction to remove this segment of RNA by exon skipping results in nuclear retention of the transcript. This mechanism for inhibiting RNA expression can be overcome by the HIV translocation protein, REV, (5, 15, 64) or engineered suppressors of mutations, e.g., U1 snRNA containing sequence complementary to mutant 5'ss (18, 33, 86). A second factor affecting RNA processing is the proximity of the major splice donor site to the pA signal. In the HIV genome, the pA signal within the 5' long terminal repeat is located immediately downstream of the transcription start site and upstream of the major 5'ss (2). In this orientation, U1 snRNA binds to the 5'ss and suppresses the upstream pA, allowing formation of the full-length transcript. However, placing this 5'ss site further from this pA signal reduces expression of the full-length transcript because it is truncated at the now-activated upstream cleavage-pA site (3). Persistent U1 snRNA binding to a site in proximity to the pA signal may account for the observation that a cryptic or an unpaired 5'ss within the terminal exon of an mRNA also prevents cytoplasmic accumulation of that mRNA, such as within the mouse polyomavirus, the BPV, and the U1A gene (23, 29, 37).

We reasoned that directing a modified U1 snRNA to a unique sequence within the terminal exon of a target gene would reduce the amount of target RNA accumulating in the cytoplasm. The reduction in gene expression would occur as a consequence of U1 snRNA binding either by interfering with the splicing reaction, inhibiting the cleavage-pA reaction, or blocking nucleo-cytoplasmic transport. Thus, the sequence of the human U1 snRNA gene was modified to specifically complement coding sequence in the targeted transgenes coding for CAT, β -Gal, or GFP (eGFP; Clontech). The magnitude, specificity, adaptability, and persistence of the U1 snRNA-based inhibition were assessed by measuring the reduction in levels of transgene RNA and protein following transient and stable transfection of the modified U1 snRNA vectors and transgene expression constructs.

MATERIALS AND METHODS

Abbreviations. The following abbreviations have been used in this work: 5'ss, 5' splice sites; 70K, 70,000 molecular weight; β -Gal, beta-galactosidase; BPV, bovine papillomavirus; CAT, chloramphenicol acetyltransferase; FACS, fluorescence-activated cell sorter; GFP, green fluorescent protein; GAPDH, glyceraldehyde-3-phosphate dehydrogenase; GTC, guanidinium thiocyanate containing 7 μ l of β -mercaptoethanol per 100 ml (17); HIV, human immunodeficiency virus; MOPS, morpholinepropanesulfonic acid; nt, nucleotides; pA, polyadenylation; PAP, poly (A) polymerase; PBS, phosphate-buffered saline; RFU, relative log fluorescent units; RSV, Rous sarcoma virus; SDS, sodium dodecyl sulfate; SET buffer, 1% SDS-1 mM EDTA-10 mM Tris buffer; SV40, simian virus 40; TK, thymidine kinase; UTR, untranslated region.

U1 targeting constructs. The parental recombinant U1 snRNA gene (63) consists of the five snRNA-specific enhancer elements in the 315-bp promoter, the U1 coding sequence, and a unique 3' termination sequence (Fig. 1A, panel i). The wild-type U1 snRNA will be referred to herein as U1 snRNA. Modified constructs will be identified as U1 antitarget gene followed by the first base number of targeted sequence, e.g., U1 anti- β -Gal1800. The target numbering begins from the AUG translation start codon.

U1 antitarget vectors were created by PCR-mutagenesis of the 5' sequence, between bases +1 and +10, which normally complements the 5' splice donor. The 5' (mutagenic) primers (Table 1 and Fig. 1A, panel i) contain a proximal *Bgl*II restriction site (underlined) for insertion into position -8 bp in the U1 promoter. The 3' (selection) primer (5' AGTGCCAAGCTTGCATGCCAGCA GGTC 3') extends through the U1 termination sequence and into the pUC18 polylinker, terminating with a *Hind*III site. A base change (underlined) was made to destroy a *Pst*I site proximal to the *Hind*III site to allow selection against

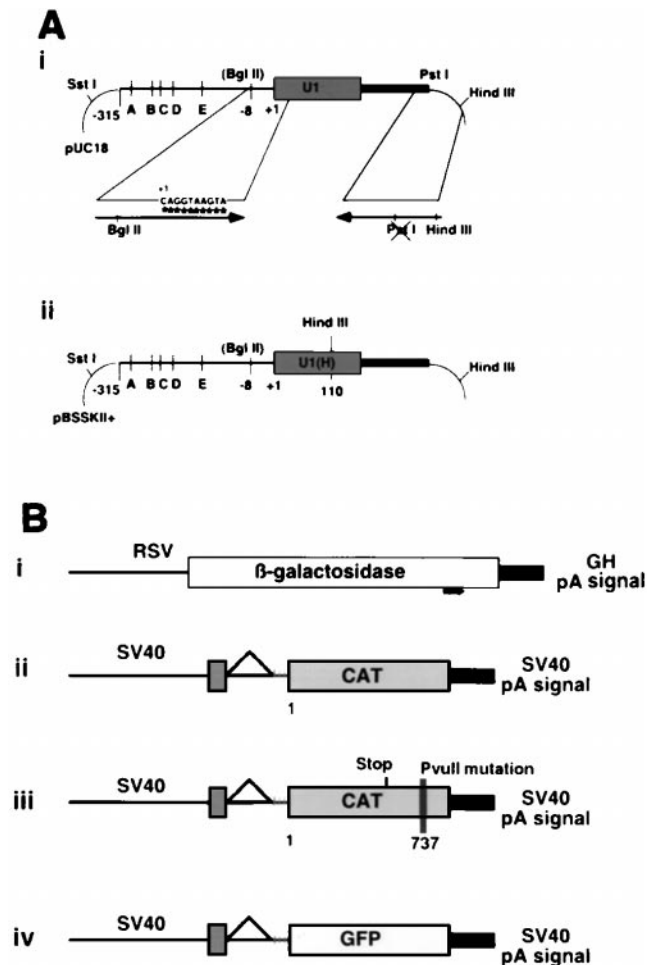


FIG. 1. (A) U1 snRNA locus. (i) Parental U1 snRNA construct with enhancer elements A through E. (ii) Map of the U1(H) construct. The arrows show the specific PCR primers used to introduce the mutations. (B) Target expression vectors. The pOB4 family of constructs has a single splice unit in which a cassette containing a triple stop unit (vertical lines) and the reporter gene are included in the terminal exon. (i) RSV β -Gal is a single exon construct; (ii) pOB4CAT; (iii) pOB4CAT(PvuII 737); (iv) pOB4GFP.

plasmids containing the original gene. The PCR product was digested with a combination of *Bgl*II, *Hind*III, and *Pst*I. The resulting clones were selected by the absence of the *Pst*I site. The same strategy was used to adapt U1 BPV and U1BPV* Δ loop1 (30). Because these constructs are located in an RNA expression plasmid (SP6), they had to be adapted to the U1 gene construct used for the cell expression studies. The 5'-mutagenic oligonucleotide consisted of the *Bgl*II adapter, the CAT737 recognition sequence, and an 11 bp sequence that overlapped U1 BPV and U1BPV* Δ loop1 from bp 11 to 22 (Table 1). The 3' selection oligo (5' AGT CTA GAT CTA CTT TTG AAA CTC CAG AAA GTC AGG GGA AAG CGC GAA CG 3') consisted of 18 bp that overlapped U1 BPV and U1BPV* Δ loop1 at bp 165 to 183 (in italic type), followed by the U1 poly(A) sequence (in boldface type) and the *Xba*I site (underlined). The PCR-derived fragments were inserted into the *Bgl*II and *Xba*I site of the U1 gene, producing U1antiCAT737a, which is identical to U1anti737, and U1antiCAT737 Δ 70K. All constructs were verified by sequencing.

A second series of constructs were engineered to distinguish stable expression of U1 antitarget transcripts from the endogenous U1 snRNA transcripts. These U1 snRNA constructs contain a *Hind*III site introduced into loop III, a non-functional component of the U1 snRNA gene (Fig. 1A, panel ii) (9, 31a, 59), and are distinguished by the use of U1(H) in their construct names. To perform this step, the U1 antitarget constructs were subcloned into pBSSK II+ utilizing the *Sst*I and *Hind*III restriction sites flanking the locus. An internal *Hind*III site was

TABLE 1. U1 snRNA constructs used to inactivate the β -Gal, CAT, and GFP target genes

Construct name(s)	Target sequence	Whole sequence ^a
U1 snRNA	CAGGTAAGTA	Not applicable
U1anti β -gal 1800	CAGTTCTGTA	5'GGCCCAAGATCTCATAACAGAACTGGCAGG3'
U1antiCAT 488	CAGTTTCATC	5'GGCCCAAGATCTCAGATGAACCTGGCAGG3'
U1antiCAT 568	CAGTTTCATC	5'GGCCCAAGATCTCAGATGAACCTGGCAGG3'
U1antiGFP 490	CCGACAAGCA	5'GGCCCAAGATCTCATGCTTGTCCGGCAGG3'
U1antiCAT 737	CAGAAATTCG	5'CCCAAGATCTCACGAATTTCTGGCAGGGGAGATACC3'
U1antiCAT 737PvuII	CAGCTGTATA	5'CCCAAGATCTCATATACAGCTGGCAGGGGAGATACC3'
U1anti737a and U1antiCAT737 Δ 70K	CAGAAATTCG	5'CCCAAGATCTCACGAATTTCTGGCAGGGGAGATACC3'

^a Underlined bases indicate the *Bgl*II restriction site used to insert the mutagenized DNA into the context of the U1 snRNA expression vectors. The last three sequences have an additional 9 bp at the 3' end (italicized) which is complementary to the U1 gene from bp 14 to 22.

then created within the constructs by single-stranded site-directed mutagenesis (45) using the following primer: 5' GCGATTCCCAAGCTTGGGAAC TCG 3'.

In vivo expression constructs. Several reporter genes were used to demonstrate the activity of the U1 antigene constructs. The RSV β -gal expression vector has the RSV promoter from pRSV2CAT (27) driving expression of the β -Gal gene (32) and terminates with the bovine growth hormone pA signal (68). There are no splicing elements in this construct (Fig. 1B, panel i).

The expression vector pOB4CAT (4) contains the SV40 enhancer-promoter, an untranslated SV40 exon, a single intron, a second exon containing stop codons in each reading frame (triple stop), the CAT gene, and the SV40 early pA site (Fig. 1B, panel ii). A second CAT expression vector pOB4CAT737PvuII, was created to evaluate the specificity of U1 targeting vectors (Fig. 1B, panel iii). It contains six mutated nucleotides at +737 bp of the vector located in the 3' UTR upstream of the SV40 pA signal. Seven bases (in boldface type) of the original sequence (5'GAATGGCAGAAATTCGCCGG3') were replaced to generate the mutant sequence (5'GAATGGCAGCTGTATACCGG3') containing a diagnostic *Pvu*II site (underlined). This was performed by internal PCR mutagenesis of the pOB4CAT vector using a 5' oligonucleotide, 5' TTAAACGTGGCCAATA TGGACAAC 3', that incorporated a *Bal*I site (underlined) and the 3' oligonucleotide, 5' CTCGAGTCCGGTATACAGCTGCCATTCATC 3', containing the mutagenic sequence (in boldface type) and a terminal *Xho*I site (underlined). The *Bal*I/*Xho*I-digested PCR fragment was cloned into an upstream unique *Bal*I and downstream *Xho*I site, rendered unique by prior destruction of the second upstream *Xho*I site present in the original pOB4CAT sequence.

The eGFP expression vector (pOB4eGFP) was derived from the pOB4CAT vector by substitution of the eGFP gene (Clontech) for the CAT gene (Fig. 1B, panel iv). Initially the unique *Xba*I site downstream of the triple stop and upstream of CAT was replaced with a *Bgl*II site. The *Xho*I site located at the 3' end of the SV40 enhancer was then replaced with an *Xba*I site, making the *Xho*I site at the 3' end of the CAT sequence unique. The eGFP gene was then inserted as a *Bam*HI-*Sal*I fragment into the *Bgl*II/*Xho*I sites.

Cell culture and transfection. NIH 3T3 fibroblasts were grown and passaged every 3 days in F12 medium containing 5% fetal calf serum with 2 mM glutamine, 1% nonessential amino acids, 100 U of penicillin per ml, and 100 μ g of streptomycin per ml. Transfection was performed using a calcium phosphate precipitate protocol (75). Transient transfections were performed with 10 μ g of U1 DNA, 2.0 μ g of reporter DNA and 1 μ g of TK-luciferase DNA. Three 100-mm-diameter plates or three 35-mm-diameter wells of six-well plates (Falcon) were used for each experimental group, with at least three transfections per data point. Analysis was performed on the cell extract harvested 48 h following the transfection.

Stable cotransfection experiments utilized 10 μ g of U1 construct, 2.0 μ g of target gene, and 1 μ g of SV2Neo selection plasmid. Transformants were selected with G418 (200 μ g/ml) for 2 weeks. Individual clones were picked, and the remaining colonies on each plate were pooled and expanded. Sequential stable transfection experiments were performed with 10 μ g of target gene DNA and 1 μ g of SV2Neo selection DNA. Transformants were selected with G418 (200 μ g/ml) for 2 weeks to obtain clones, one of which was used in all subsequent experiments. U1(H) antitarget DNA (10 μ g) was subsequently transfected with 1 μ g of a TK-hygromycin selection plasmid into this cell line. After two weeks, individual clonal populations were selected and expanded under the dual antibiotic selection for later analysis. The remaining colonies on each plate were pooled and expanded.

RNA extraction and analysis. Total cellular RNA was extracted in 700 μ l or 2 ml of Trizol (BRL) from 35- or 100-mm-diameter confluent plates, respectively, as per manufacturer's protocol with the exception of an additional precipitation step. The RNA pellet was dissolved in 300 μ l of GTC (guanadine

thiocyanate containing 7 μ l of β -mercaptoethanol per 100 ml [17]) and precipitated overnight with 300 μ l of isopropanol at -20° C, dried, and resuspended in H₂O.

Nuclear and cytoplasmic RNA fractions were obtained from 10 to 12 confluent 100-mm-diameter plates. The cells were lysed with reticulocyte swelling buffer according to previously established methods (24). The cytoplasmic fraction was extracted in 1 \times SET buffer containing proteinase K (10 μ g/ml) and resuspended in 100 to 200 μ l of diethyl pyrocarbonate-H₂O as previously described (17). The nuclear fraction was extracted a second time in reticulocyte swelling buffer, dispersed in 2 ml of GTC, extracted with acid phenol (17), and resuspended in 50 μ l of H₂O.

Northern analysis utilized 5 to 10 μ g of RNA separated in 7% formaldehyde-1X MOPS-1% agarose gel for 255 V-h. The RNA was then transferred to a nylon-reinforced nitrocellulose membrane (Schleicher and Schuell) by capillary action and UV cross-linked twice at 1,200 μ J. Hybridization was performed for 12 h at 42 $^{\circ}$ C with a final concentration of radioactive probe between 3 \times 10⁶ and 5 \times 10⁶ counts per ml of hybridization solution.

Direct RNase protection was performed with [α -³²P]rUTP uniformly labeled probes transcribed from either the T7 or T3 bacteriophage promoter in linearized pBSSK II+ (Stratagene) plasmids. The probe was hybridized to 10 μ g of test RNA or tRNA in hybridization buffer. The sample was digested with crude T₁-T₂ RNase (60 U/ml) at 30 to 34 $^{\circ}$ C for 1.5 to 2 h (50), denatured, and separated on a 6% denaturing acrylamide gel.

Transgene analysis. β -Gal enzyme activity analysis was performed on the cell extract from one confluent well of a six-well plate. The cells were lysed in 500 μ l of 0.1% SDS for 5 min, and 150 μ l of supernatant was used in each reaction mixture (65). A colorimetric stain for β -Gal activity was performed on cells from parallel wells of the transfection experiment used in the assays for enzyme activity. The staining reaction was terminated after 1 h.

CAT was extracted by lysing cells in 1 \times reporter lysis buffer (Promega). The fluor-diffusion assay was performed with 10 to 50 μ l of extract using 100,000 cpm of ³H-acetyl coenzyme A (16, 69). CAT activity was normalized to luciferase activity by mixing 10 to 20 μ l of cell extract with 50 μ l of luciferin substrate (Promega) at room temperature and immediately measuring luminescence in a Monolith 2001 luminometer (Analytical Luminescence Laboratory, Inc.) for 10 s.

Fluorescence microscopy was performed with an IMT4 Olympus inverted microscope using an eGFP optimized filter set (chroma, 41017; excitation wavelength, 470 or 40 nm emission wavelength, 525 or 500 nm; dichroic, 495LP). FACS analysis was performed on GFP expressing cultures trypsinized to a single cell suspension. The cells were washed twice in PBS and resuspended at 3 \times 10⁵ to 5 \times 10⁵ cells per ml in PBS. The cells were excited at 480 nm (argon laser), and fluorescence was recorded with a 500-nm long-pass filter on a Becton Dickinson FACS Calibur Cytometer. The effect of the U1 antitarget construct was assessed by the fluorescence index of the sample. This value was calculated as the product of the percentage of the cell population that exceeded the fluorescence intensity of the control cells and the mean fluorescence intensity of this population.

RESULTS

The U1 snRNA targeting vectors were expressed from the endogenous U1 snRNA gene that utilizes a polymerase II promoter and a U1 snRNA-specific termination sequence. Modifications were made to U1 snRNA from +1 to +10, the 5' ss recognition sequence, to produce the U1 antitarget vector to a specific RNA target. In addition a 6-bp change was in-

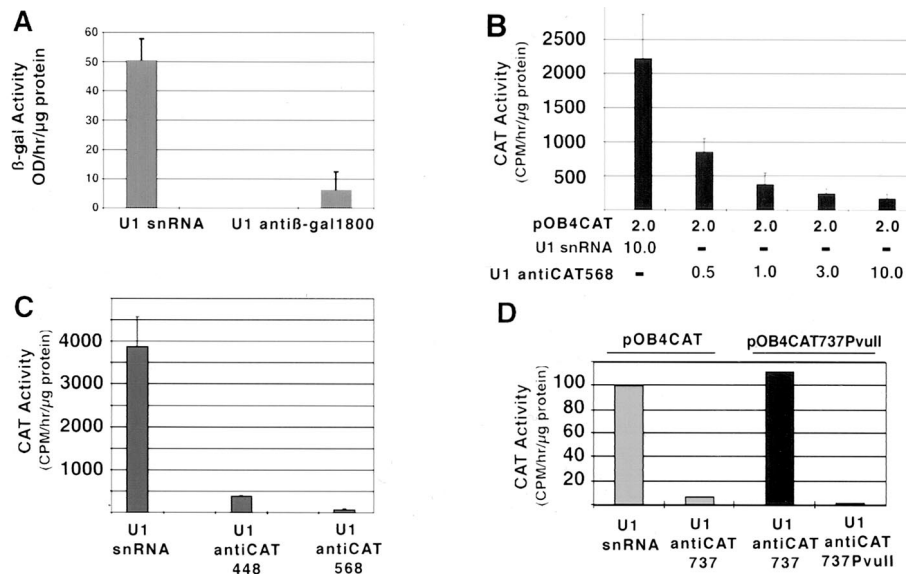


FIG. 2. (A) Reduction in β -Gal activity from three separate transient U1 anti- β -Gal-RSV β -Gal cotransfection experiments. (B) Titration of various amounts of pOB4CAT to 10 μ g of U1 anti-CAT568, yielding approximate molar ratio of CAT to U1 anti-CAT of 4:1, 2:1, 2:3, and 1:5 respectively. (C) Reduction of CAT enzyme activity by U1 anti-CAT448 and anti-CAT568 using cotransfection. (D) Sequence-specific reduction of CAT activity in transient U1 anti-CAT-pOB4CAT cotransfection experiments. pOB4CAT was used in lanes 1 and 2, and pOB4CAT 737PvuII was used in lanes 3 and 4. The U1 snRNA constructs were as follows: lane 1, U1 snRNA; lane 2, U1 anti-CAT737; lane 3, U1 anti-CAT737; lane 4, U1 anti-CAT737PvuII. These constructs were transiently cotransfected with TK-luciferase construct into NIH 3T3 cells. Error bars, standard deviations.

serted by site-directed mutagenesis into loop III of the U1 snRNA gene to distinguish the modified U1 snRNA transcript from the endogenous U1 snRNA in cultured cells. Three expression plasmids, each with a reporter as the terminal exon, were used to demonstrate the inhibitory effects of the modified U1 snRNA targeting vectors in intact cells. U1 antitarget vectors were initially tested in transient cotransfection with the reporter genes. To determine the persistence of the inhibitory effect, stable cotransfection experiments were performed with the modified U1 snRNA vector and target. Then, to approximate inhibition of an endogenous gene, sequential stable transfections were performed in which the target gene's activity had been established prior to introduction of the U1 antitarget vector. Inhibition of target gene expression was assessed by measurements of protein activity and mRNA levels. Finally, the specificity and a possible inhibitory mechanism(s) of the U1 antitarget vector have been investigated.

Reduction of transgene expression in transient-cotransfection experiments. The RSV β -Gal reporter gene was cotransfected with either U1 snRNA or U1 anti- β -Gal1800. The U1 anti- β -Gal vector reduced β -Gal enzyme activity by >90% compared to cells transfected with U1 snRNA (Fig. 2A). Parallel plates stained for β -Gal protein expression ranged in intensity from dark to light blue in both the control and test cultures. An average of 25 (\pm 2) β -Gal-positive cells per high-power field was observed in U1 snRNA cotransfections (values in parentheses are standard deviations unless otherwise noted), while cotransfection with U1 anti- β -Gal reduced β -Gal expression to 3 (\pm 1) cells per high-power field (data not shown). These results demonstrated that a modified U1 snRNA could qualitatively and quantitatively reduce protein expression from a targeted gene.

Since our goal was to target the terminal exon of selected genes containing multiple exons, the two-exon-unit expression vector pOB4CAT (4), in which the CAT gene is the terminal exon, was used. The pOB4CAT expression vector was cotransfected with U1 anti-CAT targeted to either nt 448 to 457 or nt 568 to 577 of the CAT mRNA sequence. A titration experiment of the CAT reporter to U1 antitarget vector was performed with U1 anti-CAT568 (Fig. 2B). The amount of reporter construct in the transfection was kept constant, and the amount of U1 anti-CAT568 vector varied from a ratio of 4:1 to 1:5. It was observed that inhibition of CAT expression by U1 anti-CAT568 was maximal at a ratio of 1:5. This ratio was used for subsequent experiments to demonstrate the effectiveness of U1 anti-CAT constructs targeted to randomly selected areas in the CAT mRNA sequence. U1 anti-CAT448 and U1 anti-CAT568 vectors inhibited CAT enzyme activity to 5 to 10% of controls (Fig. 2C).

The specificity of the U1 anti-CAT vector for a target sequence was assessed by directing a U1 anti-CAT vector to noncoding sequence in the 3' UTR of the pOB4CAT reporter, altering the targeted sequence, and then directing a new U1 anti-CAT vector to the altered sequence. The inhibitory effect of U1 anti-CAT737 vector is shown against the parent pOB4CAT and against the mutated pOB4CAT737PvuII reporter transgenes (Fig. 2D). U1 anti-CAT737 inhibited the expression of CAT protein by 90% when targeted to pOB4CAT transfected cells but was ineffective when targeted to the mutated pOB4CAT737PvuII reporter. However, the inhibitory effect was reestablished when U1 anti-CAT737PvuII was targeted to the mutated reporter. This experiment demonstrates that the inhibitory effect of the U1 antitarget vector is dependent on

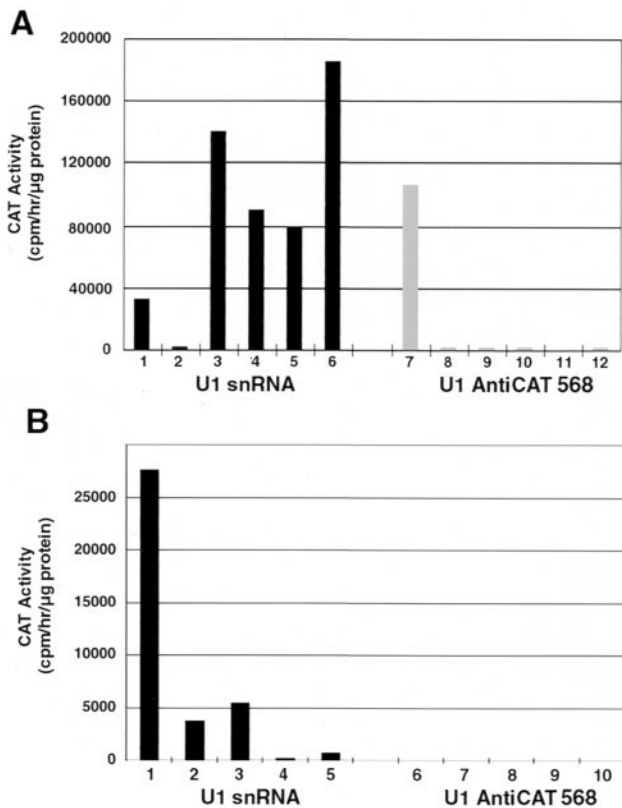


FIG. 3. (A) Reduction of CAT activity from clonally expanded stable U1 anti-CAT568/pOB4CAT cotransfection experiments. Bars 1 to 6 represent the U1 snRNA-transfected CAT-expressing cells. Bars 7 to 12 represent the U1 anti-CAT transfected CAT-expressing cells. (B) CAT activity from a clonal cell line derived by stable pOB4CAT and subsequently transfected with U1 antiCAT568. Bars 1 to 5 represent the U1 snRNA-transfected clones, and bars 6 to 10 represent the U1 anti-CAT-transfected clones.

the hybrid formed between U1 antitarget RNA and the complementary sequence in the target mRNA.

Reduction of transgene expression in stable transfection experiments. To demonstrate the persistence of this inhibitory effect on a target transcript, cells were cotransfected with the pOB4CAT vector, SV2Neo, and either U1 anti-CAT568 or U1 snRNA. After G418 selection, six randomly picked clones were analyzed. The CAT activity of the U1 snRNA-transfected clones ranged between 33,000 and 140,000 cpm/h/μg of protein, with a single clone having an activity of 2,100 cpm/h/μg of protein, while the CAT activity of the U1 anti-CAT-transfected clones ranged between 1,050 and 2,040 cpm/h/μg of protein, with a single clone having an activity of 105,000 cpm/h/μg of protein (Fig. 3A). In addition, CAT enzyme activity from pools of the remaining U1 snRNA-transfected clones was 22,800 ± 3,000 cpm/h/μg of protein, and that of U1 anti-CAT568 was 9,600 ± 2,200 cpm/h/μg of protein, consistent with the data obtained from the individual clones. Since each clone represents a different set of integration events with respect to both CAT and the U1 anti-CAT vector, it is difficult to compare individual populations. The pooled cells represent a larger cross-section of the integration events, but there remains the question of simultaneous incorporation of both genes into the same cell.

To develop a system in which both genes are represented in the cells, U1 antitarget vectors were introduced into cells in which the reporter gene had previously been inserted. An established pOB4CAT-expressing stable cell line derived from a single positive clone was subsequently transfected with either U1 snRNA or U1 anti-CAT568, and five randomly selected individual clones were expanded from both. CAT enzyme activity in control clones ranged between 82 and 3,200 cpm/h/μg of protein (Fig. 3B). CAT activity in the U1 anti-CAT-transfected clones was undetectable.

The GFP reporter was chosen as a target because we could assess the U1 antitarget activity in living cells using FACS analysis and fluorescence microscopy. Using a similar sequential transfection protocol, a single GFP-expressing clone was used to establish a cell line that was subsequently transfected with either U1 snRNA or U1 anti-GFP. The inhibitory effect was assessed by fluorescence microscopy (Fig. 4A) and quantitated using FACS analysis (Fig. 4B). Cells transfected with U1 snRNA were of uniform bright green fluorescence (Fig. 4A, panel 3). In U1 anti-GFP transfections, some of the cells were equally fluorescent as the control cells, a smaller percentage were less fluorescent and approximately half were not visibly fluorescent (Fig. 4A-4).

The visual impression of reduced GFP expression in U1 anti-GFP transfected cells was confirmed by FACS analysis of the cells. The autofluorescence background, established with NIH 3T3 cells (Fig. 4B, panel 1), was less than 1.5 RFU. The GFP-transfected cell line (Fig. 4B, panel 2) had a mode distribution of 3.2 RFU, 2 log units greater than untransfected cells. Pools of multiple colonies transfected with U1(H) snRNA (Fig. 4B, panel 3) showed a single peak at 3.2 RFU, while pools from U1 anti-GFP transfections (Fig. 4B, panel 4) were seen as three peaks: 50% low fluorescence (<2 RFU), 25% intermediate (2 to 3 RFU) and 25% high (≥3 RFU). A fluorescence index was established to reflect the inhibition by U1 antiGFP vector (Table 2). This index emphasizes the magnitude of signal generated by the GFP-transfected cell lines over nontransfected cells. The reduction in GFP signal strength in the polyclonal population of U1(H) anti-GFP-transfected cells is approximately 70%. Clones from this transfection were developed for subsequent RNA analysis.

Clonal populations of U1 snRNA- and U1 anti-GFP-transfected GFP-expressing cells were randomly selected, expanded, and analyzed by FACS (Fig. 4C). The FACS profiles of untransfected cells (clone A) and GFP parental cells (clone B) were similar to those of the cells presented in Fig. 4B. The cells from the U1(H) snRNA transfections (clones C and D) had a strong narrow peak of fluorescence at approximately 3.0 RFU,

TABLE 2. Fluorescence of a pooled population of GFP-expressing cells as determined by flow cytometry

Sample	Description	% in M2 window ^a	Mean intensity	Fluorescence index
1	Control (nontransfected)	0.16	333	52
2	Parental cells (nontransfected)	94.5	1,804	171,000
3	Parental + U1(H) snRNA	92.5	1,873	170,000
4	Parental + U1(H) antiGFP	60.5	851	51,000

^a M2 is the window in the FACS scan where the fluorescent signal exceeds the background of GFP negative cells. (See Fig. 4B.)

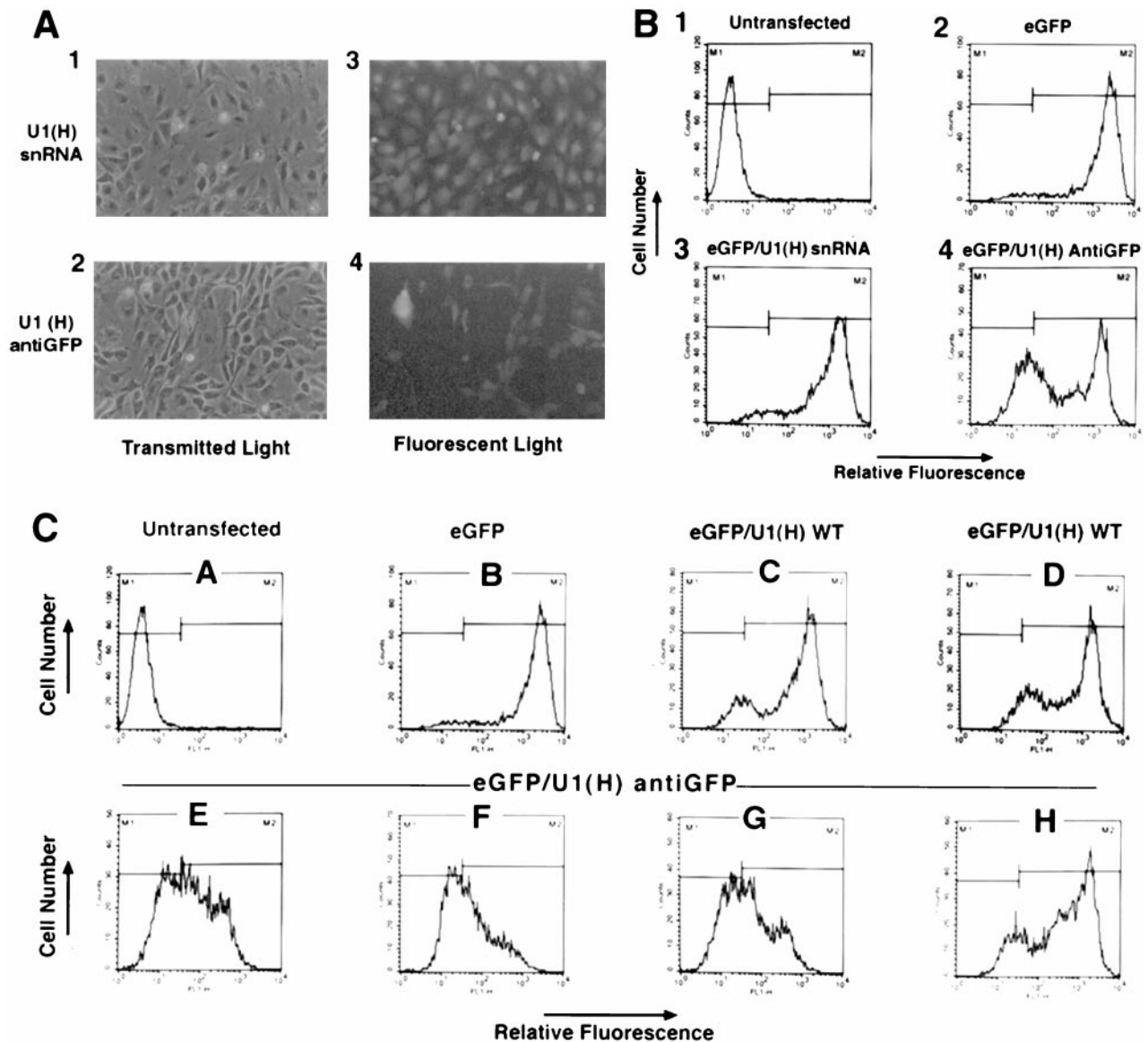


FIG. 4. (A) Micrographs showing the reduction of stable GFP expression in NIH 3T3 cells by U1(H) anti-GFP. U1 Panels 1 and 3, U1 snRNA; panels 2 and 4, U1 anti-GFP. (B) FACS analysis of the cells shown in panel A shows the reduction in the number and intensity of the fluorescent cells containing the U1 anti-GFP construct. Panel 1, untransfected NIH 3T3 cells; panels 2 to 4, untransfected pOB4GFP stable line; panel 3, pOB4GFP and U1 snRNA; panel 4, pOB4GFP and U1 anti-GFP. (C) FACS of clonal lines stably transfected with control or U1 anti-GFP constructs. Panels: A, untransfected NIH 3T3 cells; B to H, pOB4GFP-expressing cells either untransfected (B) or transfected with U1(H) snRNA (C and D) or U1(H) anti-GFP (E to H).

slightly less intense than that of clone B, and in addition had a smaller second peak of fluorescence at 1.5 RFU. In contrast, cells from clones E, F, and G, transfected with U1 anti-GFP had significantly lower fluorescence intensity, with a broad distribution from 1 to 3 RFU. Cells from clone H, which were only minimally inhibited by microscopy, showed a FACS profile of a strong peak at 3 RFU and a small peak at 1.5 RFU. The fluorescence indices for clones C to H are shown in Table 3. The GFP signal strength in clones E, F, and G is approximately 10% of that of clones C and D, whereas clone H is minimally inhibited. Clones A to H were used for subsequent RNA analysis.

TABLE 3. Fluorescence of an isolated clonal population of GFP-expressing cells as determined by flow cytometry

Sample	Description	% in M2 window ^a	Mean intensity	Fluorescence index
C	Parental + U1(H) snRNA	89.6	1,014	90,900
D	Parental + U1(H) snRNA	92.0	1,119	102,900
E	Parental + U1(H) antiGFP	57.5	200	11,500
F	Parental + U1(H) antiGFP	51.6	183	9,450
G	Parental + U1(H) antiGFP	53.5	180	9,640
H	Parental + U1(H) antiGFP	86.8	954	82,800

^a M2 is the window in the FACS scan where the fluorescent signal exceeds the background of GFP negative cells (see Fig. 4C).

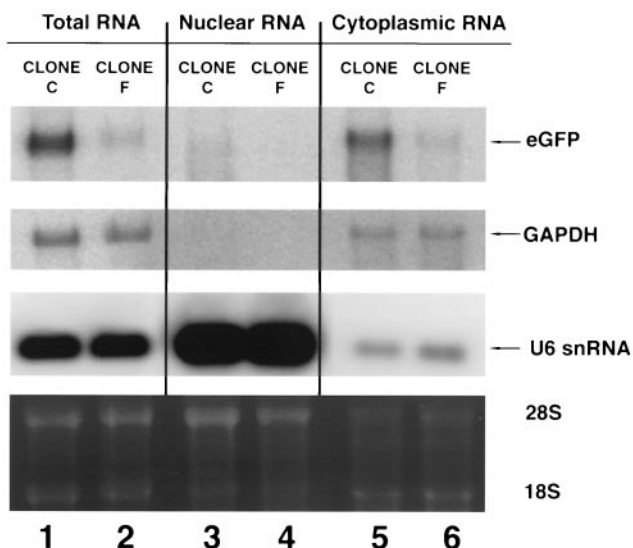


FIG. 5. Total RNA from an expanded clonal population of GFP-expressing cells stably transfected with U1(H) snRNA and U1(H) anti-GFP derived from the experiment shown in Fig. 4C. Clone C, U1(H) snRNA; clone F, U1(H) anti-GFP. GFP mRNA was normalized to GAPDH. U6 snRNA was used to show the efficiency of nuclear and cytoplasmic RNA extraction. The lower panel shows the ethidium bromide-stained agarose gel.

Mechanism of U1 antitarget vector inhibition of transgene expression. Northern analysis was performed on total, nuclear, and cytoplasmic mRNA harvested from U1 snRNA (clone C) and U1 anti-GFP (clone F) clones derived from cells shown in Fig. 4B to determine if there were evidence of nuclear accu-

mulation of the targeted GFP RNA (Fig. 5). There was major reduction in the level of total GFP RNA in cells from clone F relative to clone C that correlated with the degree of GFP fluorescence. The high amount of U6 RNA in the nuclear compartment demonstrates that the RNA extraction procedure effectively separated the RNA into nuclear and cytoplasmic compartments. The level of GFP mRNA was decreased in both the nuclear and cytoplasmic compartments in clone F, suggesting that inhibition of GFP expression was not occurring by a mechanism in which bound U1 anti-GFP impedes the export of the GFP transcript to the cytoplasm.

To assess whether the effect of U1 anti-GFP was due to inhibition of the 3' cleavage step of mRNA processing, an RNase protection assay was performed using a 500-bp probe spanning the pA signal site. The diagram in Fig. 6 shows the predicted 350-bp band when GFP mRNA is terminated at the pA site. Interference with the cleavage reaction will result in a fully protected 500-bp band. As expected all GFP expressing clones had the predicted 350-bp band in the cytoplasmic compartment. Clone B, the GFP parental population, had a strong 350-bp and a weaker 500-bp band in the nuclear RNA. Since this 500-bp band is not present in the cytoplasm, it is unlikely to represent nonspecific protection of the hybridization probe. Instead, it most likely represents a small proportion of unprocessed GFP mRNA within the nucleus. Clone H, a U1(H) anti-GFP-transfected population with minimal inhibition of GFP expression, showed both 350- and 500-bp bands in the same proportion as did clone B. Clones E, F, and G, with lower fluorescence levels, had undetectable levels of the 350-bp band, consistent with the Northern blot data seen in Fig. 5, and no evidence of the 500-bp band. This experiment suggests that

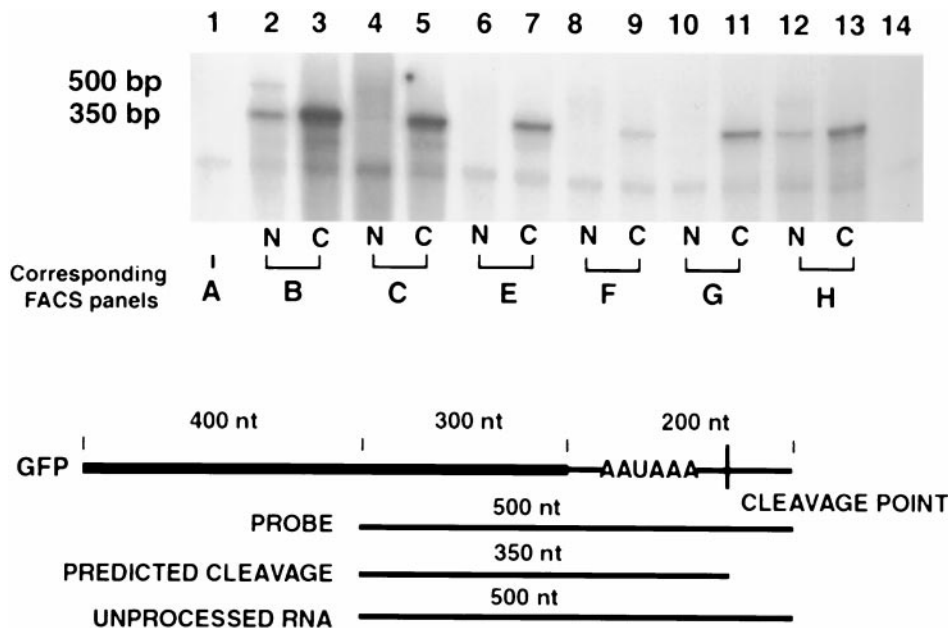


FIG. 6. RNase protection assay showing the relative amounts of GFP transgenes in nuclear and cytoplasmic mRNA from clonal populations of stably GFP-expressing cells subsequently transfected with U1(H) snRNA or U1(H) anti-GFP. The properly terminated transgene is seen as a 350-nt band, and read-through mRNA is seen as a 500-bp protected band. The two controls are in lane 1 (total NIH 3T3 RNA) and lane 14 (tRNA). Lanes 2, 4, 6, 8, 10, and 12 contain nuclear RNA, and lanes 3, 5, 7, 9, 11, and 13 control cytoplasmic RNA. The following clones are those described in the FACS analysis in Fig. 4C: clone B, GFP-expressing cells (lanes 2 and 3); clone C, U1(H) snRNA (lanes 4 and 5); and clones E to H, U1(H) anti-GFP (in lanes 6 and 7, 8 and 9, 10 and 11, and 12 and 13, respectively).

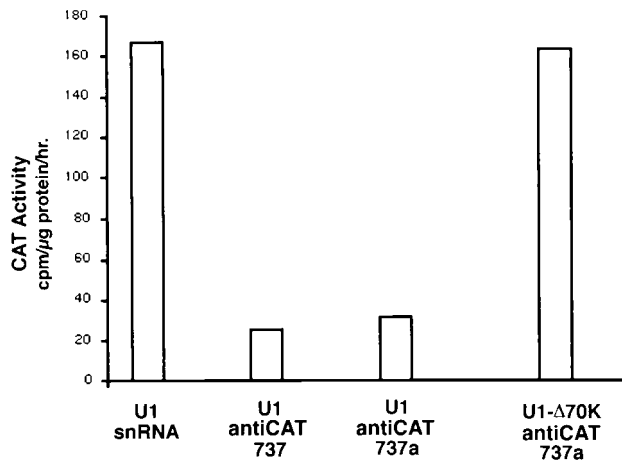


FIG. 7. Loss of inhibitory activity of the U1 anti-CAT737 construct when the 70K binding domain is destroyed. The constructs used to study the role of the 70K binding protein and PAP in vitro (30) were adapted to express the modified U1 transcripts from the U1 promoter. The control for an intact 70K binding domain (U1 anti-CAT737a) is identical to the U1 antiCAT737 analyzed in Fig. 2. These constructs were used in transient-cotransfection experiments with pOB4CAT and TK-luciferase in NIH 3T3 cells.

either the inhibitory effect of U1 anti-GFP is not at the cleavage step of mRNA processing, or if it is, that the uncleaved transcript is rapidly degraded, precluding its detection by our experimental protocol.

Another possible mechanism of the U1 antitarget gene is inhibition of pA of the targeted transcript due to the inhibition of PAP by the U1 snRNA-associated U1 70K protein. To test this potential mechanism, a mutation was placed within the binding site for the U1 70K protein to produce the construct U1 anti-CAT737Δ70K. Transient cotransfections of pOB4CAT with U1 snRNA, U1 anti-CAT737 (presented previously), U1 anti-CAT737a (a control for the U1 Δ70 designed construct [see Materials and Methods]) and U1 anti-CAT737Δ70K were performed in NIH 3T3 cells. A TK-luciferase gene construct was cotransfected as an internal control to normalize transfection efficiency. As shown in Fig. 7, both U1 anti-CAT737 and U1 anti-CAT737a significantly reduce CAT activity compared to U1 snRNA, as previously demonstrated. However, U1 anti-CAT737Δ70K showed no inhibitory effect on CAT activity. These results suggest that U1 70K protein plays an important role in the inhibitory mechanism of a modified U1 antitarget gene expression, possibly by interference with pA. It also indicates that the reduction in gene expression by the U1 anti-target vector is unlikely to be attributable to an antisense mechanism.

The steady-state content of the transcript arising from the transfected U1 anti-GFP relative to endogenous U1 snRNA transcript was assessed by RNase protection. The U1-derived transcripts are fully protected by the U1 hybridization probe producing a 177-bp band (Fig. 8). The endogenous U1 snRNA is cleaved at the internal *Hind*III site (position +110), yielding a 110-bp band corresponding to the 5' fragment and a 67-bp 3' fragment (not shown on gel). In all the clones, endogenous and transfected U1 snRNA transcripts were observed primarily in the nuclear compartment. Quantitative analysis showed that

the U1 transcripts represented between 1 and 8% of the endogenous U1 snRNA levels. The number of clones analyzed was insufficient to observe a correlation between the levels of the U1 anti-GFP transcripts and inhibition of GFP expression.

DISCUSSION

The effectiveness of RNA inhibition strategies in vivo has been variable. Successful inhibition by conventional antisense or ribozyme has required extensive empirical testing of several constructs prior to selecting the optimal site within the target mRNA (21, 47, 72). This suggests that the most important obstacle in reducing mRNA expression from a specific gene is access to the targeted sequence. Another problem is the inability to bring target and effector into close proximity (12, 49). Since all mRNAs are posttranscriptionally modified by 5' capping, splicing, 3' cleavage, and pA, agents that can interfere with processing of a specific transcript have the potential to be an effective anti-RNA strategy. The ubiquitous snRNAs partition to the nucleus and colocalize with pre-mRNA that is undergoing the processing steps required for maturation and export to the cytoplasm (28, 35, 56). Several groups have already demonstrated the ability of U1 and tRNA to present ribozymes (42, 46, 57–60, 85) and U7 snRNAs to deliver antisense sequences (79) to a target RNA by taking advantage of

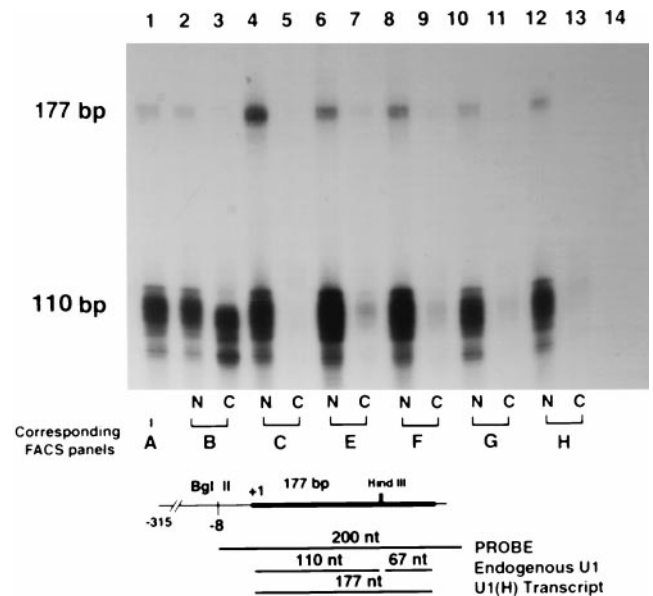


FIG. 8. RNase protection assay showing the relative amount of U1 antitarget RNA in the nuclear (N) and cytoplasmic (C) mRNA from clonal populations of stably GFP-expressing cells subsequently transfected with U1 snRNA or U1(H) anti-GFP (Fig. 4C). The U1(H) snRNA transcript is a 177-nt band, and the endogenous U1 snRNA transcript is a 110-nt band. The two controls are in lane 1 (total NIH 3T3 RNA) and lane 14 (tRNA). Lanes 2, 4, 6, 8, 10, and 12 contain nuclear RNA, and lanes 3, 5, 7, 9, 11, and 13 contain cytoplasmic RNA. The following clones are those described in the FACS analysis in Fig. 4C: clone B, GFP-expressing cells (lanes 2 and 3); clone C, U1(H) snRNA (lanes 4 and 5); clones E to H, U1(H) anti-GFP (in lanes 6 and 7, 8 and 9, 10 and 11, and 12 and 13, respectively). The appearance of a U1 transcript in lane 3 (clone B cytoplasm) probably represents contamination of the sample with nuclear RNA, as suggested by its smaller size.

cellular compartmentalization of splicing factors with nascent RNA.

U1 snRNA was chosen to target mRNA because it may overcome these two problems. Previously, the intrinsic capability of U1 snRNA to bind 5'ss of pre-mRNA and to reduce expression from a gene containing a cryptic 5'ss in the terminal exon have been demonstrated. Despite its short hybridization domain, the U1 snRNA within the U1 snRNP complex has the ability to recognize and bind to the splice donor sequences distributed throughout a transcript, overcoming the problem of access to regions within a target transcript. In addition it should colocalize with pre-mRNA, overcoming the problem of proximity. Once the 5'ss sequence is bound, the transcript can only be exported from the nucleus after the intron containing the 5'ss is excised (15, 70). We reasoned that if U1 snRNP was not released from an mRNA because of the absence of a 3' splice acceptor site and splicing cascade, the targeted mRNA would not successfully complete RNA processing and would be destroyed. Such a situation would occur if the U1 snRNA was targeted to a sequence in the terminal exon.

The modified U1 antitarget vectors examined displayed sequence specificity in inhibiting gene expression of three targeted transgenes by as much as 95%. Specific reduction of protein and RNA levels of transiently and stably expressed reporter genes was obtained. The conclusions from these experiments are that U1 snRNA transgenes can be targeted to inhibit mRNA from a gene simultaneously cotransfected or separately transfected into cells. The inhibition of the GFP and CAT genes in stable transfections was persistent in these experiments. The reduction of GFP expression was maintained in stably transfected cells for at least 1 month in culture. In addition, recent experiments indicate that the U1 antitarget vector can reduce endogenous gene expression, such as the expression of osteocalcin and the osteoblastic transcription factor *cbfa1* in osteoblastic cells (unpublished data).

The U1 antitarget transcripts are localized to the nucleus (Fig. 6) and inhibit the majority of targeted mRNA from accumulating in the nucleus and cytoplasm. RNA that escapes the inhibitory action of U1 antitarget vectors appears to have proper 3' end formation and is translated into a functional protein. The inhibition of the CAT gene was dependent on the hybrid formed between the U1 antitarget vector and the target sequence (Fig. 2D). The inhibition was demonstrated at many sites within the domain of the terminal exon of the CAT target as well as a randomly selected GFP sequence. Even without a functional splice unit, β -Gal was also inhibited by the U1 antitarget construct.

Mammalian cells are not affected by the presence of naturally occurring pseudo-U1 genes containing aberrant splice recognition domains (52, 53, 84). Since the cells stably transfected with the U1 antitarget vectors were observed to have normal growth parameters and normal morphology, we have concluded that the modified U1 snRNA vectors are much like the pseudo-U1 snRNA genes. The levels of U1 antitarget transcripts achieved in these cells did not appear to cause critical nonspecific reductions in the level of other genes necessary for cell function. Such an untoward effect may be uncovered when primary cells undergoing a complex differentiation pathway are presented with a U1 antitarget vector. This is a valid criticism of any strategy that targets RNA and one that may be resolved

only by examining the majority of the expressed genes of the targeted cells, for example, through microarray analysis.

The mechanism of inhibition of target transgene activity by the U1 antitarget vectors is still uncertain. Our initial expectation, based on our prior experience with certain splice donor mutations of the COL1A1 gene (70, 78), was nuclear sequestration in a splicing SC-35 domain and subsequent degradation of the target mRNA (14, 38, 76). We postulated that persistent binding of the U1 snRNA to the mutant donor site could account for failure of the transcript to proceed through the SC-35 domain and that our U1 snRNA targeted transcripts would suffer a similar fate. This does not appear to be the case in these experiments, because we found no evidence of nuclear accumulation of the targeted mRNA (Fig. 5 and 6).

Studies with the mouse polyomavirus and BPV demonstrated that U1 snRNP-5'ss complex binding of a cryptic splice donor site located within 500 bp of the cleavage-pA signal reduces the expression of either transcript (20, 23, 36, 54). The postulated mechanism for this inhibitory effect, based on these *in vitro* experiments, involves the interaction of U1 70K protein with PAP to inhibit pre-mRNA polyadenylation (30, 31, 40, 83). Our *in vivo* results using the U1 antiCAT Δ 70K constructs are consistent with these findings. In the RNase protection experiments, proper 3' end formation of GFP mRNA was demonstrated in the U1 anti-GFP clones with reduced expression of GFP (Fig. 6). These results suggest that the interaction of the U1 snRNP may interfere with only pA rather than both cleavage and polyadenylation and are consistent with data demonstrating the effects of an upstream 5'ss with pA (81). In contrast, studies with 5'ss downstream of the pA site show effects on both cleavage and pA steps (1-3). The U1 anti-CAT Δ 70K experiment also suggested that the reduction of gene expression by the modified U1 construct does not result from an antisense mechanism, because if this were the case, the deletion of U1 70K binding site sequence should not destroy the inhibitory effect of U1 antitarget vector. In contrast to the results shown above, targeting sequences within the first exon or intron failed to reduce CAT activity (unpublished data). This further indicates that U1 antitarget vector can only reduce gene expression when a sequence within the terminal exon is targeted.

We conclude that the molecular mechanism for the inhibitory effects of U1 antitarget described here is most likely related to inhibition of pA. The multiprotein complex that mediates this reaction includes the cleavage and polyadenylation stimulating factor, cleavage stimulating factor CstF, cleavage factors I and II, and PAP. The U1 snRNP 70K protein independently binds to and inhibits the PAP component of the complex. Although the U1 snRNP U1A protein stimulates PAP activity *in vitro* (55, 66), it has been shown to inhibit pA of the U1A mRNA transcript both *in vitro* and in intact cells, (11, 29-31, 82), suggesting a broader role in its regulation of the pA reaction. At this point it is unclear which mechanism is critical to the activity of the U1 target RNA. All that can be stated with certainty is that cleavage of modified U1-targeted RNA is occurring correctly and mRNA transcripts in both the nuclear and cytoplasmic compartment are low. These observations suggest the process of pA is impaired, leading to a transcript more susceptible to degradation (7, 13, 25).

There are likely to be many variables that will influence the

ability of U1 antitarget vectors to effectively down regulate expression of a target gene. One factor may be the level of expression of the target gene. Another factor would be the level of expression of the U1 antitarget gene. We observed that U1(H) anti-GFP transcripts are appropriately localized in the nucleus of stably transfected cells and inhibit gene expression for the duration of our experiments. The expression of the U1 antitarget RNA varied from 1 to 8% of the level of endogenous U1 snRNA genes. In the limited number of samples examined, there did not appear to be a correlation between the level of U1 snRNA expression and the degree of inhibition of the target. Delivering the U1 antitarget vectors within the context of a retrovector may improve the strength and consistency of expression. Finally, because the U1 snRNA strategy appears to act within the nuclear compartment of the cells, its RNA action might be complemented with a ribozyme or antisense mRNA strategy that is active on RNA localized in the cytoplasmic compartment of the cell.

ACKNOWLEDGMENTS

This work was supported by Public Health Service grant AR 30426 from the National Institute of Arthritis and Musculoskeletal and Skin Diseases, National Institute of Health, to D.W.R. and grant GM57286 from the National Institute of General Medical Sciences to S.I.G.

We thank G. Carmichael and B. Graveley for their contributions in shaping the course of these experiments.

REFERENCES

- Ashe, M. P., A. Furger, and N. J. Proudfoot. 2000. Stem-loop 1 of the U1 snRNP plays a critical role in the suppression of HIV-1 polyadenylation. *RNA* **6**:170–177.
- Ashe, M. P., P. Griffin, W. James, and N. J. Proudfoot. 1995. Poly(A) site selection in the HIV-1 provirus: inhibition of promoter-proximal polyadenylation by the downstream major splice donor site. *Genes Dev.* **9**:3008–3025.
- Ashe, M. P., L. H. Pearson, and N. J. Proudfoot. 1997. The HIV-1 5' LTR poly(A) site is inactivated by U1 snRNP interaction with the downstream major splice donor site. *EMBO J.* **16**:5752–5763.
- Baker, C. C. 1990. An improved chloramphenicol acetyltransferase expression vector system for mapping transcriptional and post-transcriptional regulatory elements in animal cells, p. 75–86. *In* K. K. Alitalo et al. (ed.), *Recombinant systems in protein expression*. Elsevier Science Publishers B. V., Amsterdam, The Netherlands.
- Barksdale, S. K., and C. C. Baker. 1995. The human immunodeficiency virus type 1 Rev protein and the Rev-responsive element counteract the effect of an inhibitory 5' splice site in a 3' untranslated region. *Mol. Cell. Biol.* **15**:2962–2971.
- Berget, S. M. 1995. Exon recognition in vertebrate splicing. *J. Biol. Chem.* **270**:2411–2414.
- Bernstein, P., and J. Ross. 1989. Poly(A), poly(A) binding protein and the regulation of mRNA stability. *Trends Biochem. Sci.* **14**:373–377.
- Bertrand, E., D. Castanotto, C. Zhou, C. Carbonnelle, N. S. Lee, P. Good, S. Chatterjee, T. Grange, R. Pictet, D. Kohn, D. Engelke, and J. J. Rossi. 1997. The expression cassette determines the functional activity of ribozymes in mammalian cells by controlling their intracellular localization. *RNA* **3**:75–88.
- Birnstiel, M. L. (ed.). 1988. *Structure and function of major and minor small nuclear ribonucleoprotein particles*. Springer-Verlag, Berlin, Germany.
- Blencowe, B. J., J. A. Nickerson, R. Issner, S. Penman, and P. A. Sharp. 1994. Association of nuclear matrix antigens with exon-containing splicing complexes. *J. Cell Biol.* **127**:593–607.
- Boelens, W. C., E. J. Jansen, W. J. van Venrooij, R. Stripecke, I. W. Mattaj, and S. I. Gunderson. 1993. The human U1 snRNP-specific U1A protein inhibits polyadenylation of its own pre-mRNA. *Cell* **72**:881–892.
- Bramlage, B., E. Luzi, and F. Eckstein. 1998. Designing ribozymes for the inhibition of gene expression. *Trends Biotechnol.* **16**:434–438.
- Burkard, K. T., and J. S. Butler. 2000. A nuclear 3'-5' exonuclease involved in mRNA degradation interacts with poly(A) polymerase and the hnRNA protein Np13p. *Mol. Cell. Biol.* **20**:604–616.
- Carter, K. C., D. Bowman, W. Carrington, K. Fogarty, J. A. McNeil, F. S. Fay, and J. B. Lawrence. 1993. A three-dimensional view of precursor messenger RNA metabolism within the mammalian nucleus. *Science* **259**:1330–1335.
- Chang, D. D., and P. A. Sharp. 1989. Regulation by HIV Rev depends upon recognition of splice sites. *Cell* **59**:789–795.
- Chireux, M., J. F. Raynal, and M. J. Weber. 1994. Performance and limits of the mixed-phase assay for chloramphenicol acetyltransferase at low [³H]acetyl-CoA concentration. *Anal. Biochem.* **219**:147–153.
- Chomczynski, P., and N. Sacchi. 1987. Single-step method of RNA isolation by acid guanidinium thiocyanate-phenol-chloroform extraction. *Anal. Biochem.* **162**:156–159.
- Cohen, J. B., S. D. Broz, and A. D. Levinson. 1993. U1 small nuclear RNAs with altered specificity can be stably expressed in mammalian cells and promote permanent changes in pre-mRNA splicing. *Mol. Cell. Biol.* **13**:2666–2676.
- Cole-Strauss, A., K. Yoon, Y. Xiang, B. C. Byrne, M. C. Rice, J. Gryn, W. K. Holloman, and E. B. Kmiec. 1996. Correction of the mutation responsible for sickle cell anemia by an RNA-DNA oligonucleotide. *Science* **273**:1386–1389.
- Cooke, C., H. Hans, and J. C. Alwine. 1999. Utilization of splicing elements and polyadenylation signal elements in the coupling of polyadenylation and last-intron removal. *Mol. Cell. Biol.* **19**:4971–4979.
- Dropulic, B., and K. T. Jeang. 1994. Gene therapy for human immunodeficiency virus infection: genetic antiviral strategies and targets for intervention. *Hum. Gene Ther.* **5**:927–939.
- Fiering, S., M. A. Bender, and M. Groudine. 1999. Analysis of mammalian cis-regulatory DNA elements by homologous recombination. *Methods Enzymol.* **306**:42–66.
- Furth, P. A., W. T. Choe, J. H. Rex, J. C. Byrne, and C. C. Baker. 1994. Sequences homologous to 5' splice sites are required for the inhibitory activity of papillomavirus late 3' untranslated regions. *Mol. Cell. Biol.* **14**:5278–5289.
- Genovese, C., and D. Rowe. 1987. Analysis of cytoplasmic and nuclear messenger RNA in fibroblasts from patients with type I osteogenesis imperfecta. *Methods Enzymol.* **145**:223–235.
- Gerstel, B., M. F. Tuite, and J. E. McCarthy. 1992. The effects of 5'-capping, 3'-polyadenylation and leader composition upon the translation and stability of mRNA in a cell-free extract derived from the yeast *Saccharomyces cerevisiae*. *Mol. Microbiol.* **6**:2339–2348.
- Giles, R. V., C. J. Ruddell, D. G. Spiller, J. A. Green, and D. M. Tidd. 1995. Single base discrimination for ribonuclease H-dependent antisense effects within intact human leukaemia cells. *Nucleic Acids Res.* **23**:954–961.
- Gorman, C. M., G. T. Merlino, M. C. Willingham, I. Pastan, and B. H. Howard. 1982. The Rous sarcoma virus long terminal repeat is a strong promoter when introduced into a variety of eukaryotic cells by DNA-mediated transfection. *Proc. Natl. Acad. Sci. USA* **79**:6777–6781.
- Grimm, C., E. Lund, and J. E. Dahlberg. 1997. In vivo selection of RNAs that localize in the nucleus. *EMBO J.* **16**:793–806.
- Gunderson, S. I., K. Beyer, G. Martin, W. Keller, W. C. Boelens, and L. W. Mattaj. 1994. The human U1A snRNP protein regulates polyadenylation via a direct interaction with poly(A) polymerase. *Cell* **76**:531–541.
- Gunderson, S. I., M. Polycarpou-Schwarz, and I. W. Mattaj. 1998. U1 snRNP inhibits pre-mRNA polyadenylation through a direct interaction between U1 70K and poly(A) polymerase. *Mol. Cell* **1**:255–264.
- Gunderson, S. I., S. Vagner, M. Polycarpou-Schwarz, and I. W. Mattaj. 1997. Involvement of the carboxyl terminus of vertebrate poly(A) polymerase in U1A autoregulation and in the coupling of splicing and polyadenylation. *Genes Dev.* **11**:761–773.
- Hamm, J., N. A. Dathan, D. Scherly, and I. W. Mattaj. 1990. Multiple domains of U1 snRNA, including U1 specific protein binding sites, are required for splicing. *EMBO J.* **9**:1237–1244.
- Herman, G. E., W. E. O'Brien, and A. L. Beaudet. 1986. An *E. coli* beta-galactosidase cassette suitable for study of eukaryotic expression. *Nucleic Acids Res.* **14**:7130.
- Hitomi, Y., K. Sugiyama, and H. Esumi. 1998. Suppression of the 5' splice site mutation in the Nagase analbuminemic rat with mutated U1snRNA. *Biochem. Biophys. Res. Commun.* **251**:11–16.
- Horowitz, D. S., and A. R. Krainer. 1994. Mechanisms for selecting 5' splice sites in mammalian pre-mRNA splicing. *Trends Genet.* **10**:100–106.
- Huang, S., and D. L. Spector. 1992. U1 and U2 small nuclear RNAs are present in nuclear speckles. *Proc. Natl. Acad. Sci. USA* **89**:305–308. (Erratum, **89**:4218–4219.)
- Huang, Y., and G. C. Carmichael. 1996. Role of polyadenylation in nucleocytoplasmic transport of mRNA. *Mol. Cell. Biol.* **16**:1534–1542.
- Huang, Y., and G. G. Carmichael. 1996. A suboptimal 5' splice site is a cis-acting determinant of nuclear export of polyomavirus late mRNAs. *Mol. Cell. Biol.* **16**:6046–6054.
- Johnson, C., D. Primorac, M. McKinstry, J. McNeil, D. Rowe, and J. Lawrence. 2000. Tracking COL1A1 RNA in osteogenesis imperfecta: splice-defective transcripts initiate transport from the gene but are retained within the SC35 domain. *J. Cell Biol.* **150**:417–431.
- Klebba, C., O. G. Ottmann, M. Scherr, M. Pape, J. W. Engels, M. Grez, D. Hoelzer, and S. A. Klein. 2000. Retrovirally expressed anti-HIV ribozymes confer a selective survival advantage on CD4+ T cells in vitro. *Gene Ther.* **7**:408–416.
- Klein Gunnewiek, J. M., R. I. Hussein, Y. van Aarsen, D. Palacios, R. de Jong, W. J. van Venrooij, and S. I. Gunderson. 2000. Fourteen residues of

- the U1 snRNP-specific U1A protein are required for homodimerization, cooperative RNA binding, and inhibition of polyadenylation. *Mol. Cell. Biol.* **20**:2209–2217.
41. **Konforti, B. B., M. J. Koziolkiewicz, and M. M. Konarska.** 1993. Disruption of base pairing between the 5' splice site and the 5' end of U1 snRNA is required for spliceosome assembly. *Cell* **75**:863–873.
 42. **Koseki, S., T. Tanabe, K. Tani, S. Asano, T. Shioda, Y. Nagai, T. Shimada, J. Ohkawa, and K. Taira.** 1999. Factors governing the activity in vivo of ribozymes transcribed by RNA polymerase III. *J. Virol.* **73**:1868–1877.
 43. **Kren, B. T., R. Metz, R. Kumar, and C. J. Steer.** 1999. Gene repair using chimeric RNA/DNA oligonucleotides. *Semin. Liver Dis.* **19**:93–104.
 44. **Kumar, M., and G. G. Carmichael.** 1998. Antisense RNA: function and fate of duplex RNA in cells of higher eukaryotes. *Microbiol. Mol. Biol. Rev.* **62**:1415–1434.
 45. **Kunkel, T. A., K. Bebenek, and J. McClary.** 1991. Efficient site-directed mutagenesis using uracil-containing DNA. *Methods Enzymol.* **204**:125–139.
 46. **Kuwabara, T., M. Warashina, M. Orita, S. Koseki, J. Ohkawa, and K. Taira.** 1998. Formation of a catalytically active dimer by tRNA(Val)-driven short ribozymes. *Nat. Biotechnol.* **16**:961–965.
 47. **Lapte, A. V., Z. Lu, A. Colige, and D. J. Prockop.** 1994. Specific inhibition of expression of a human collagen gene (COL1A1) with modified antisense oligonucleotides. The most effective target sites are clustered in double-stranded regions of the predicted secondary structure for the mRNA. *Biochemistry* **33**:11033–11039.
 48. **Lear, A. L., L. P. Eperon, I. M. Wheatley, and I. C. Eperon.** 1990. Hierarchy for 5' splice site preference determined in vivo. *J. Mol. Biol.* **211**:103–115.
 49. **Lee, N. S., E. Bertrand, and J. Rossi.** 1999. mRNA localization signals can enhance the intracellular effectiveness of hammerhead ribozymes. *RNA* **5**:1200–1209.
 50. **Lichtler, A., N. L. Barrett, and G. G. Carmichael.** 1992. Simple, inexpensive preparation of T1/T2 ribonuclease suitable for use in RNase protection experiments. *BioTechniques* **12**:231–232.
 51. **Ludwig, J., M. Blaschke, and B. S. Sproat.** 1998. Extending the cleavage rules for the hammerhead ribozyme: mutating adenosine 15.1 to inosine 15.1 changes the cleavage site specificity from N16.2U16.1H17 to N16.2C16.1H17. *Nucleic Acids Res.* **26**:2279–2285.
 52. **Lund, E.** 1988. Heterogeneity of human U1 snRNAs. *Nucleic Acids Res.* **16**:5813–5826.
 53. **Lund, E., and J. E. Dahlberg.** 1984. True genes for human U1 small nuclear RNA. Copy number, polymorphism, and methylation. *J. Biol. Chem.* **259**:2013–2021.
 54. **Lutz, C. S., and J. C. Alwine.** 1994. Direct interaction of the U1 snRNP-A protein with the upstream efficiency element of the SV40 late polyadenylation signal. *Genes Dev.* **8**:576–586.
 55. **Lutz, C. S., K. G. Murthy, N. Schek, J. P. O'Connor, J. L. Manley, and J. C. Alwine.** 1996. Interaction between the U1 snRNP-A protein and the 160-kD subunit of cleavage-polyadenylation specificity factor increases polyadenylation efficiency in vitro. *Genes Dev.* **10**:325–337.
 56. **Matera, A. G., and D. C. Ward.** 1993. Nucleoplasmic organization of small nuclear ribonucleoproteins in cultured human cells. *J. Cell Biol.* **121**:715–727.
 57. **Medina, M. F., and S. Joshi.** 1999. Design, characterization and testing of tRNA^{Lys}-based hammerhead ribozymes. *Nucleic Acids Res.* **27**:1698–1708.
 58. **Michienzi, A., L. Conti, B. Varano, S. Prislei, S. Gessani, and I. Bozzoni.** 1998. Inhibition of human immunodeficiency virus type 1 replication by nuclear chimeric anti-HIV ribozymes in a human T lymphoblastoid cell line. *Hum. Gene Ther.* **9**:621–628.
 59. **Michienzi, A., S. Prislei, and I. Bozzoni.** 1996. U1 small nuclear RNA chimeric ribozymes with substrate specificity for the Rev pre-mRNA of human immunodeficiency virus. *Proc. Natl. Acad. Sci. USA* **93**:7219–7224.
 60. **Montgomery, R. A., and H. C. Dietz.** 1997. Inhibition of fibrillin 1 expression using U1 snRNA as a vehicle for the presentation of antisense targeting sequence. *Hum. Mol. Genet.* **6**:519–525.
 61. **Mount, S. M., I. Pettersson, M. Hinterberger, A. Karmas, and J. A. Steitz.** 1983. The U1 small nuclear RNA-protein complex selectively binds a 5' splice site in vitro. *Cell* **33**:509–518.
 62. **Muller, U.** 1999. Ten years of gene targeting: targeted mouse mutants, from vector design to phenotype analysis. *Mech. Dev.* **82**:3–21.
 63. **Murphy, J. T., R. R. Burgess, J. E. Dahlberg, and E. Lund.** 1982. Transcription of a gene for human U1 small nuclear RNA. *Cell* **29**:265–274.
 64. **Najera, I., M. Krieg, and J. Karn.** 1999. Synergistic stimulation of HIV-1 rev-dependent export of unspliced mRNA to the cytoplasm by hnRNP A1. *J. Mol. Biol.* **285**:1951–1964.
 65. **Norton, P. A., and J. M. Coffin.** 1985. Bacterial beta-galactosidase as a marker of Rous sarcoma virus gene expression and replication. *Mol. Cell. Biol.* **5**:281–290.
 66. **O'Connor, J. P., J. C. Alwine, and C. S. Lutz.** 1997. Identification of a novel, non-snRNP protein complex containing U1A protein. *RNA* **3**:1444–1455.
 67. **Ohkawa, J., and K. Taira.** 2000. Control of the functional activity of an antisense RNA by a tetracycline-responsive derivative of the human U6 snRNA promoter. *Hum. Gene Ther.* **11**:577–585.
 68. **Pfarr, D. S., L. A. Rieser, R. P. Woychik, F. M. Rottman, M. Rosenberg, and M. E. Reff.** 1986. Differential effects of polyadenylation regions on gene expression in mammalian cells. *DNA* **5**:115–122.
 69. **Purschke, W. G., and P. K. Muller.** 1994. An improved fluor diffusion assay for chloramphenicol acetyltransferase gene expression. *BioTechniques* **16**:264–265, 268–269.
 70. **Redford-Badwal, D. A., M. L. Stover, M. Valli, M. B. McKinstry, and D. W. Rowe.** 1996. Nuclear retention of COL1A1 messenger RNA identifies null alleles causing mild osteogenesis imperfecta. *J. Clin. Invest.* **97**:1035–1040.
 71. **Robberson, B. L., G. J. Cote, and S. M. Berget.** 1990. Exon definition may facilitate splice site selection in RNAs with multiple exons. *Mol. Cell. Biol.* **10**:84–94.
 72. **Robertson, M. P., and A. D. Ellington.** 1999. In vitro selection of an allosteric ribozyme that transduces analytes to amplicons. *Nat. Biotechnol.* **17**:62–66.
 73. **Rosbash, M., and B. Seraphin.** 1991. Who's on first? The U1 snRNP-5' splice site interaction and splicing. *Trends Biochem. Sci.* **16**:187–190.
 74. **Rossi, F., T. Forne, E. Antoine, J. Tazi, C. Brunel, and G. Cathala.** 1996. Involvement of U1 small nuclear ribonucleoproteins (snRNP) in 5' splice site-U1 snRNP interaction. *J. Biol. Chem.* **271**:23985–23991.
 75. **Selden, R. F.** 1990. Introduction of DNA into mammalian cells, p. 9.1.1–9.1.9. *In* R. B. Frederick M. Ausubel, R. E. Kingston, D. D. Moore, J. G. Seidman, J. A. Smith, and K. Struhl, (ed.), *Current protocols in molecular biology*, vol. 1. Greene Publishing Associates and Wiley-Interscience, New York, N.Y.
 76. **Smith, K. P., P. T. Moen, K. L. Wydner, J. R. Coleman, and J. B. Lawrence.** 1999. Processing of endogenous pre-mRNAs in association with SC-35 domains is gene specific. *J. Cell Biol.* **144**:617–629.
 77. **Stein, C. A.** 1999. Two problems in antisense biotechnology: in vitro delivery and the design of antisense experiments. *Biochim. Biophys. Acta* **1489**:45–52.
 78. **Stover, M. L., D. Primorac, S. C. Liu, M. B. McKinstry, and D. W. Rowe.** 1993. Defective splicing of mRNA from one COL1A1 allele of type I collagen in nondeforming (type I) osteogenesis imperfecta. *J. Clin. Investig.* **92**:1994–2002.
 79. **Suter, D., R. Tomasini, U. Reber, L. Gorman, R. Kole, and D. Schumperli.** 1999. Double-target antisense U7 snRNAs promote efficient skipping of an aberrant exon in three human beta-thalassemic mutations. *Hum. Mol. Genet.* **8**:2415–2423.
 80. **Tuschl, T., M. M. Ng, W. Pieken, F. Benseler, and F. Eckstein.** 1993. Importance of exocyclic base functional groups of central core guanosines for hammerhead ribozyme activity. *Biochemistry* **32**:11658–11668. (Erratum, **33**:848, 1994.)